Application of Combustion Hot Spot Analysis to Process Furnace with Arbor Coils

Behnoush Barzegar[1], Seyed Hamed Mousavi[*1], Seyed Mohammad Ali Moosavian[2], Babak Maghbooli[3] and Hamid Reza Najafi[3]

[1]Faculty of Caspian, College of Engineering, University of Tehran, Guilan, I. R. Iran
[2]School of Chemical Engineering, College of Engineering, University of Tehran, Tehran, I. R. Iran
[3]Farayand Sabz Engineering Company, No.117, Somaye Street, Tehran, I. R. Iran

Abstract

Hot spots are among the most serious operational issues in furnaces as they may result in the destruction of tubes. Hence, it is essential to locate such hot spots precisely on the tube surfaces inside the industrial furnaces in order to secure a safe design and operation. In the current study, we have extended the model proposed by Talmor in order to precisely locate the combustion hot spots on the surface of the tubes inside process furnaces with arbor coils. These furnaces are mostly used in catalytic reforming units. The Talmor model is one of the best models for analyzing combustion hot spots on the tube surfaces of industrial furnaces. This model is developed by considering the furnace geometry and arrangement (tube arrangements and burner positions). In the current paper, we have derived and extended the equations formulated by Talmor for furnaces with arbor coil. As the second step, a specific furnace already installed in a catalytic conversion unit of a refinery has been selected for the sake of modeling. The modeling of the preceding furnace was completed using the code prepared for this purpose. The results have been used not only for analyzing the hot spots but also to model the heat flux profile inside the furnace. Upon modeling the furnace, the location of the hot spot on the 20th coil was predicted which was consistent with the experimental results.

1. Introduction

Examining the combustion zone inside a furnace and determining the heat flux originating from this zone allows one to locate the hot spots and the maximum skin temperature points of the tubes. In order to track the developments in modeling the combustion zone and the heat flux originating from that, below we have summarized the methods and models previously proposed for this purpose.

Hottel proposed the long furnace and the well stirred enclosure models. In the long furnace model, the ratio of the furnace length to its width or that of length to diameter is assumed to be very large and presumably the temperature variations in the radial direction are negligible. In the well stirred enclosure, in the completely uniform combustion chamber model we assume a total uniform composition of the combustion products. These two models are exclusively applicable to ideal situations such as those with simple geometries and uniform environments having independent spectral properties [1].

Current progress in computational methods has introduced superior models such as zonal methods and Monte Carlo techniques. Zonal methods are based on dividing the furnace into volumetric or area cells of identical physical and chemical properties (e.g., temperature, emissivity, chemical composition, etc.) after which an energy balance is written on each cell. Finally, the resulting equations are solved simultaneously in order to find the temperature and heat flux distributions. The zonal method propounded by Hottel and Sarofim was developed for absorbing media irradiating without transmission and gray gases with constant coefficients [1]. The zonal method suggested by Hottel and Cohen [2] and also that formulated by Noble [3] have been written for physical media consisting of non-gray gaseous environments with variable properties and isotropic transmission. Yuen and Takara [4]

amended the previous method to account for anisotropy in transmission, although the simultaneous solution in the presence of anisotropic transmission is still attractive. Marino presented a simple model for the control of reheating rotary furnaces in which the radiation effects between different zones and between the burners and also the convection heat transfer have been neglected [5]. Mechi and coworkers employed the zonal method in order to predict the heat flux in quadrilateral-shaped furnaces [6]. Recently, Ebrahimi and colleagues utilized the zonal method for a physical medium with emission-absorption in industrial furnaces [7]. Tan and coworkers also compared two and three-dimensional zonal methods in reheating furnaces [8].

The Monte Carlo method is also similar to zonal method and is applicable for more complex geometries. This method was first reported by Fleck [9] and also Howell and Pelmutter [10,11] and was used for investigating the one-dimensional radiation heat transfer. Steward and Cannon were the first researchers who applied this method to furnaces where they calculated the radiation heat flux in cylindrical combustion chambers. In exploiting this method, for the solution of simultaneous radiation-conduction problems in physical media and its consequences, Abed and Sacadura [13], Liu and Tiwari [14], and for three-dimensional geometries, Farmer and Howell [15] conducted investigations. Mishara and Blank applied this method as a measure of solving two-dimensional chamber with an isotropic absorption-emission radiation [16]. Zhou and coworkers put forward an emissive model based on the Monte Carlo method in order to facilitate temperature measurement [17]. Soroka compared this method with the other heat transfer methods for different geometries [18]. Maurente et al. used Monte Carlo technique to predict temperatures in cylindrical and cubic chambers [19]. Kovtanyuk et al. employed Monte Carlo experiments to simultaneously solve radiation and conduction heat transfer

in a physical medium in the presence of isotropic transmission [20].

Computational fluid dynamics (CFD) model is another numerical method. This method has been evaluated for media containing emission and for known temperature distribution inside the chamber and known flux-based boundary conditions in simultaneous solution with conduction or convection by Razzaque et al. [21,22], Chung and Kim [23], and finally Fernandes and coworkers [24,25]. Harish and Dutta used this model in an attempt to forecast the heat transfer in a reheating furnace to calculate the gas radiation heat transfer [26]. Additionally, Kim suggested a mathematical model for predicting temperature distribution and thermal flux inside a furnace with an intermediate radiation, at different temperature variations and constant absorption coefficient [27]. Hachem et al. developed a three-dimensional CFD model for industrial furnaces with a special attention to the internal hot solids [28].

All the time, new numerical methods are introduced and extended for predicting the thermal flux in combustion chamber of process heaters. In the current study, we elaborate and extend one of these methods.

2. Methods

The method employed in the current study is based on geometric ratios and was originally developed by Talmor [29]. In this model as shown in Figure 1, the thermal radiation center is assumed to be on a hypothetical axis ξ. In order to calculate the thermal flux on the tubes, constant flux loci resulting from spherical surfaces with different radii R_1 are used which leads to Equation (1) below [29]:

$$dq_x = \frac{f \cdot dQ}{4\pi \cdot R_1^2} \qquad (1)$$

Moreover, the combustion chamber is assumed to be a cone frustum with a height equal to the flame length (Figure 2).
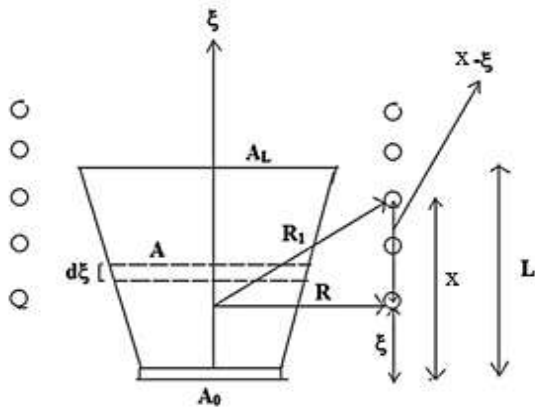
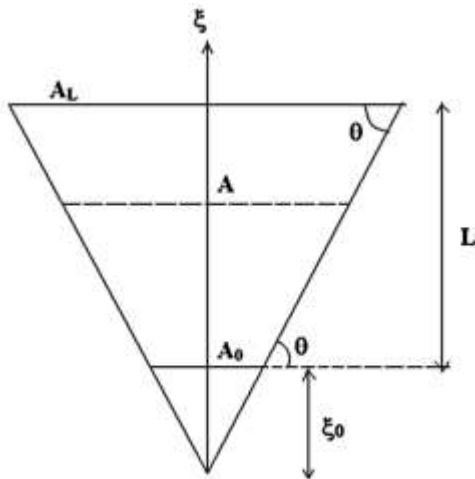**Figure1: Schematic showing the source of heat and radiation [29].**

Figure2: Schematic showing the cone-shaped by the burner flame [30].
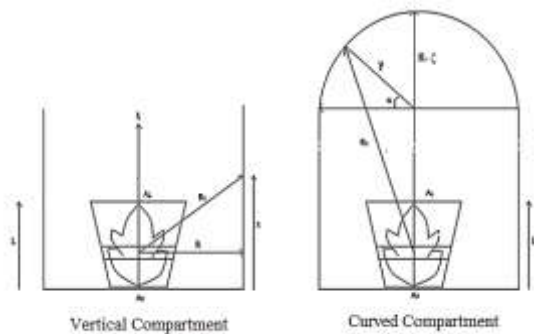

Figure3: The two compartments (vertical and curved) assumed in the furnace with arbor coil in Cartesian coordinates.

Figure 1 leads to Equations (2) and (3) and their corollaries:

$$\frac{A}{A_L} = \left[\frac{\xi+\xi_0}{L+\xi_0}\right]^2 \qquad (2)$$

$$\frac{A_L}{A_0} = \left[\frac{L+\xi_0}{\xi_0}\right]^2 \rightarrow \sqrt{\frac{A_L}{A_0}} = \frac{L+\xi_0}{\xi_0} \qquad (3)$$

$$\rightarrow \xi_0 = \frac{L}{\sqrt{\frac{A_L}{A_0}}-1}$$

Where L is calculated by the following equation [29]:

$$L = \frac{3\,K\,Q_L}{A_0 + A_L + \sqrt{A_0 A_L}} \qquad (4)$$

In cases where a gas burner is used as the thermal source we can assume constant emissivity and volumetric heat generation:

$$\frac{dQ}{dV} = const. = \frac{Q_L}{V_L} \qquad (5)$$

$$dQ = \left(\frac{dQ}{dV}\right)dV = \left(\frac{dQ}{dV}\right)A.d\xi = \left(\frac{Q_L}{V_L}\right)A.d \qquad (6)$$

Replacing Equations (2) to (6) in Equation (1), results in:

$$dq_x = \frac{fQ_L A_L (\xi+\xi_0)^2 d\xi}{4\pi V_L (L+\xi_0)^2 R_1^2} \qquad (7)$$

In order to acquire the final relation based on actual measurable parameters we have to replace the R_1 value. For this purpose, in a furnace with arbor coil, the furnace is divided into two compartments: the vertical compartment and the curved compartment; and separate equations are derived for each one.

It should be noted that the geometric parameters that were used for driving Equation (7) are the same for either horizontal or vertical tube layouts. Based on Figure 3, R_1 can be derived for each compartment and replaced for in Equation (7). The R_1 value of the vertical and the curved compartments can be stated using Equations (8) and (9), respectively:

$$R_1 = \sqrt{R^2 + (x-\xi)^2} \qquad (8)$$

$$R_1 = \sqrt{(R - \xi - y + y\sin\alpha)^2 + (y\cos\alpha)^2} \qquad (9)$$

By inserting Equations (8) and (9) in Equation (7) and integrating the resulting relations from $(q_x = 0; \xi = 0)$ to $(q_x = q_x; \xi = L)$, we end up with Equations (10) and (11) that may be used for calculating the thermal flux in the vertical and curved compartments, respectively.

$$\left(\frac{4\pi R^2 q_x}{3fQ_L}\right)\frac{1+\frac{A_L}{A_0}+\sqrt{\frac{A_L}{A_0}}}{\left(\sqrt{\frac{A_L}{A_0}}-1\right)^2} = \frac{1}{(L/R)^2} \qquad (10)$$

$$+ \frac{\frac{x}{L}+\frac{\xi_0}{L}}{(L/R)^2}\ln\frac{1+\left(\frac{L}{R}\right)^2\left(1-\frac{x}{L}\right)^2}{1+\left(\frac{L}{R}\right)^2\left(\frac{x}{L}\right)^2}$$

$$+ \frac{\left(\frac{L}{R}\right)^2\left(\frac{x}{L}+\frac{\xi_0}{L}\right)^2-1}{(L/R)^3}$$

$$\times\left[\tan^{-1}\left(\frac{L}{R}\right)\left(1-\frac{x}{L}\right)+\tan^{-1}\left(\frac{L}{R}\right)\left(\frac{x}{L}\right)\right]$$

And

$$\frac{4.\pi.R^2.q}{3.f.Q_L}\left(\frac{L}{R}\right)^2\left(\frac{1+\frac{A_L}{A_0}+\sqrt{\frac{A_L}{A_0}}}{\left(\sqrt{\frac{A_L}{A_0}}-1\right)^2}\right) = 1 +$$

$$\left(\frac{1}{L/R} + \frac{\xi_0}{L} + \frac{y}{L}(\sin\alpha-1)\right)$$

$$\times\ln\left(\frac{\left(1-\frac{L}{R}\right)^2+2\frac{y}{R}\left(\frac{y}{R}-1+\frac{L}{R}\right)(1-\sin\alpha)}{1+2\frac{y}{R}\left(\frac{y}{R}-1\right)(1-\sin\alpha)}\right)$$

$$(11)$$

$$+\left(\frac{\left(1+\frac{L}{R}\frac{\xi_0}{L}\right)^2}{\frac{y}{R}\frac{L}{R}\cos\alpha}\right.$$

$$+ \frac{2\frac{y}{R}\left(1+\frac{\xi_0}{L}\frac{L}{R}\right)(\sin\alpha-1)}{\frac{y}{R}\frac{L}{R}\cos\alpha}$$

$$\left. - \frac{2\left(\frac{y}{R}\right)^2(\sin\alpha-1+\cos\alpha^2)}{\frac{y}{R}\frac{L}{R}\cos\alpha}\right)$$

$$\times\left[\tan^{-1}\left(\frac{\left(\frac{L}{R}-1\right)+\frac{y}{R}(1-\sin\alpha)}{\frac{y}{R}\cos\alpha}\right)\right.$$

$$\left. - \tan^{-1}\left(\frac{\frac{y}{R}(1-\sin\alpha)-1}{\frac{y}{R}\cos\alpha}\right)\right]$$

3. Results

The results were obtained through the algorithm which flowchart is displayed in Figure 4. As it is evident in Figure 4, in order to begin, input values are required which are given in Tables 1 and 2. Then, using the equations expressed in this article, calculations were done and finally to calculate the skin temperature, Talmor's equations were used.

3.1. Analyzing the predicted thermal flux in the vertical and curved compartments

Dimensionless thermal flux number $((4\pi R^2 q)/(3f.Q_L))$ for each compartment versus different dimensionless flame lengths (L/R) are shown in Figure 5. As can be seen in Figure 5 (a), at $L/R<2$, that is at short flame lengths or large separations between the flame and furnace tubes, the dimensionless thermal flux number is about 0.33 and is almost independent of L/R and A_L/A_0. As these ratios increase the dimensionless thermal flux also changes significantly. However, as observable in Figure 4 this dimensionless number is a strong function of L/R and a weak function of A_L/A_0.

Figure 5 (b) indicates that at small dimensionless flame lengths, that happens when the flame is far from furnace tubes, the dimensionless thermal flux is also small and by increasing L/R and A_L/A_0 ratios this

number also rises. Again, the dependence on L/R is much more, similar to the vertical compartment.

3.2. Locating combustion hot spot and evaluating thermal and temperature distribution on the tube with hot spots

In this section we have used the modeling results to locate the hot spots inside a furnace with arbor coils. This process heater is located in a catalytic reforming unit. The furnace has 7 burners located at the furnace floor with up-firing configuration. The arbor coil is containing of 34 tubes with a surface area of 3.5×7.7753 m^2.

The center to center spacing between each two adjacent burners is 0.97 m (Figure 6). Although there are various theoretical and empirical methods available for calculating emissivity of hot gases within the firebox enclosure, but in order to simplify calculations as much as possible and avoid lengthy discussions simplest correlation was selected for calculating this parameter. Nevertheless, the accuracy of this correlation is acceptable for design and practical simulation procedures. For fuel gases with C/H ratios between 3.5 and 5.0 used Eq. (12) [29]:
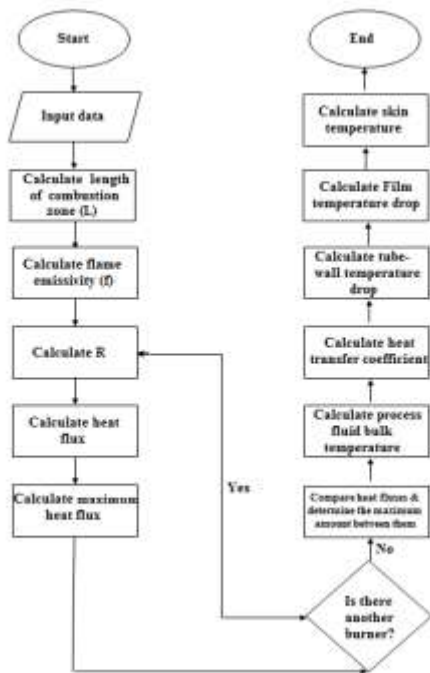
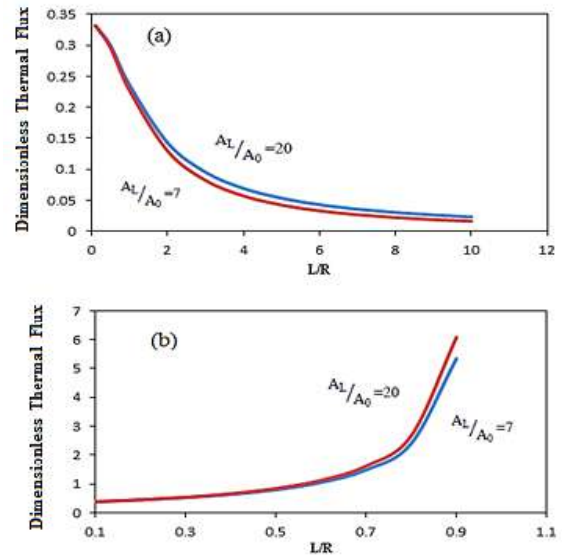**Figure4: Flowchart to locate hot spots with Talmor method**

Figure5: Dimensionless thermal flux versus dimensionless flame length of the vertical (a) and the curved (b) compartments

$$f = 0.048 \sqrt{MW} \qquad (12)$$

In Tables 1 and 2 the input data necessary for modeling the furnace are summarized:

Table1: General arrangement and basic design parameters of furnace

Properties	Value
A_0	0.31172 m^2
A_L	3.8876 m^2
Q	1416.8784 kw
K [29]	0.0028986 m^3/kw
D_o	0.1143 m
D_i	0.1022 m
l	22.7m

Table2: Properties of process fluid

Properties	Value
V	60 m/s
Mass flow rate	115842 kg/hr
MW	27.8 kg/kmol
T_{in}	477 °C

According to the developed equations for Talmor model a computational code was developed using the C++ programming

language. It was found that the maximum heat flux which was 37.4396 kW/m^2, occurs at 1.7 m from the bottom of the furnace that was predicted to be on the 20th tube. Nonetheless, the maximum permissible average heat flux for this furnace was 37.8 kW/m^2, which is slightly more than the maximum value predicted by modeling. Figure 7 (a) depicts the thermal flux distribution along the 20th tube in both compartments.

Since the furnace is symmetric, we can take advantage of the symmetry rules and determine the heat flux distribution for only one half of the furnace and apply the same distribution for the other half as well.

Figure 7 (b) illustrates the skin temperature distribution on the full length of the 20th tube. Here, we observe two maxima on the surface one of which occurs at 1.7 m

with a temperature of 525.33°C and the other at 21 m from the start of the tube length with a temperature of 571.676°C. The maximum temperature spots in Figure 8 correspond to the maximum heat flux exposure.
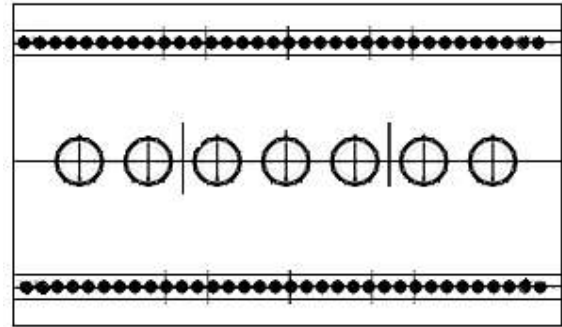

Figure 6:Top view of the furnace with arbor coil.

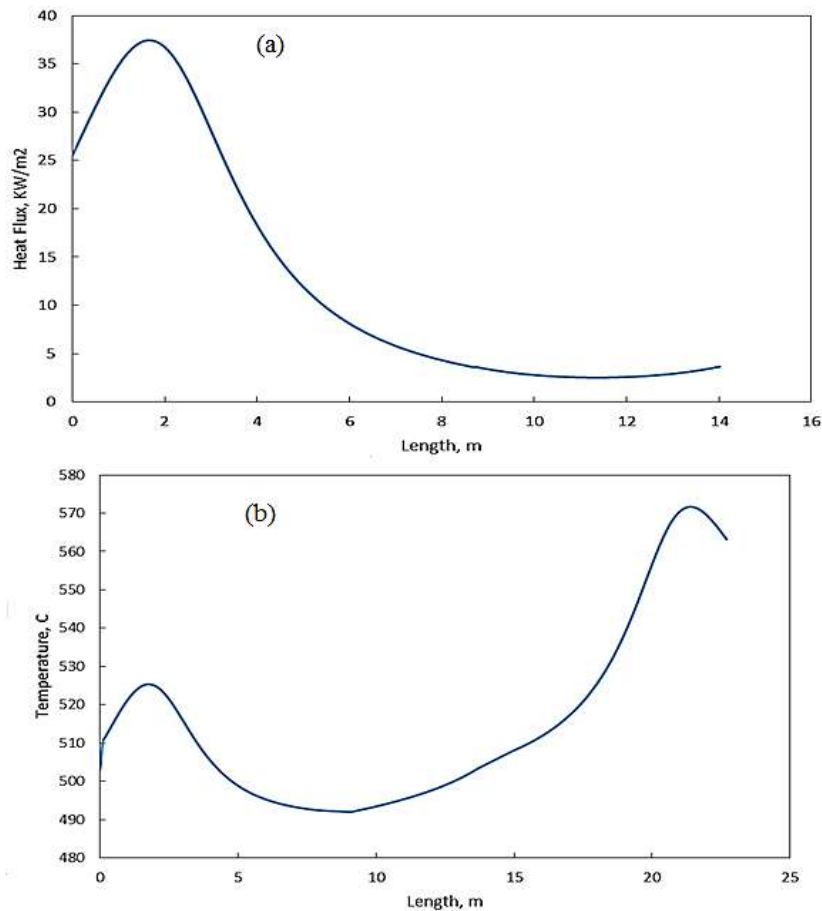**Figure7: (a) Heat flux distribution of the 20th coil; (b) Temperature distribution on the tube surface of the 20th coil. (Vertical section: (0-8.7 m and 13.9-22.6 m), curved section: (8.7-13.9 m))**
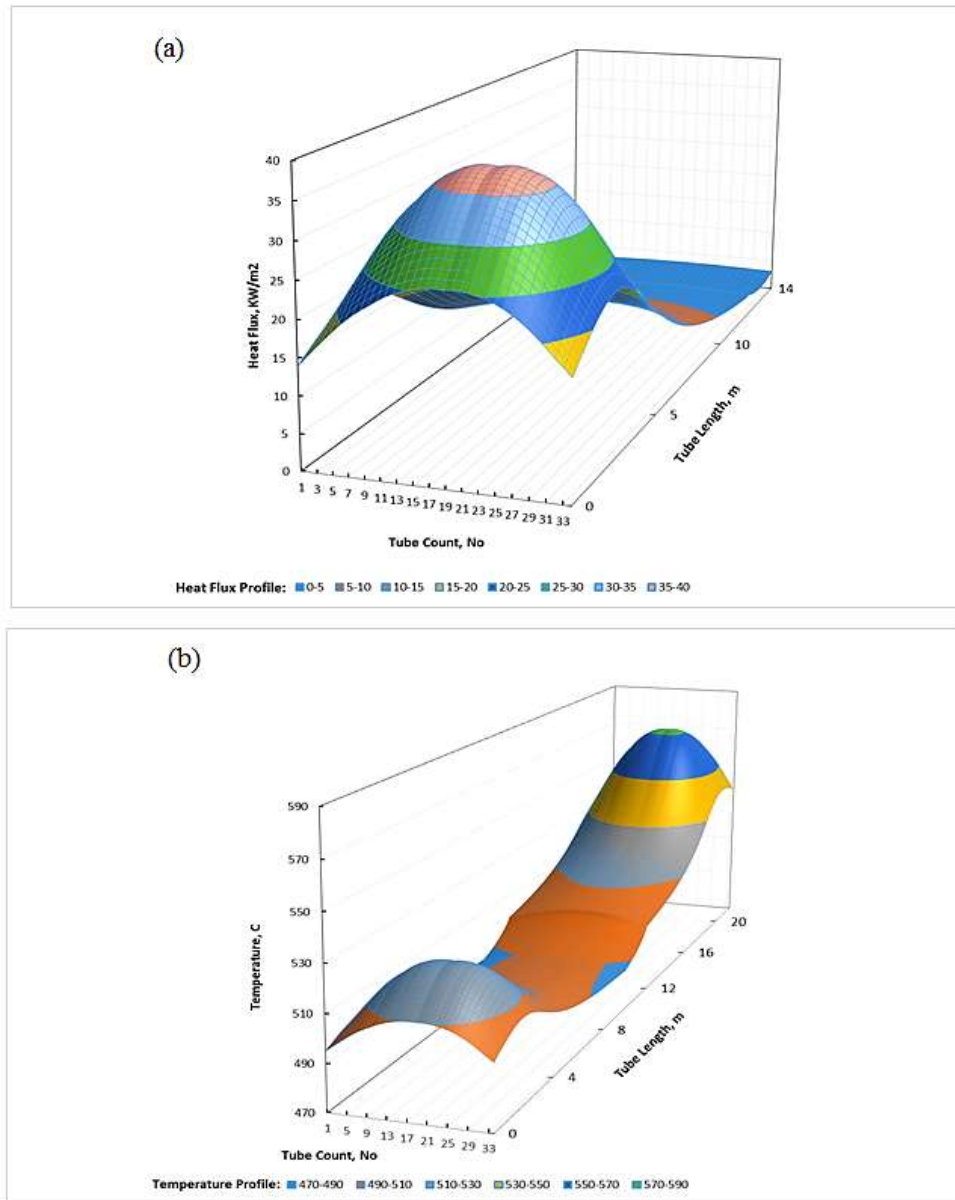
Figure8: Three-dimensional distribution of (a) thermal flux and (b) tube surface temperature for all the coils.

Table3. Comparison between the simulation and experimental results.

No. of coils	Thermocouple locations based on coil length (m)[a]	Calculated temperature (°C)	Maximum experimental temperature (°C)[b]
5	5.1	493.35	541
5	17.6	513.186	564
29	5.1	495.489	542
29	17.6	517.192	539

Note:

a: Common tube skin temperature measurement thermocouples that are welded to the tube skin in compliance with API standards

b: Measurement error is $\pm 1°\mathbf{C}$

3.3. Evaluating overall thermal and temperature distributions

Figure 8 (a) shows the overall three-dimensional heat flux distribution for all the 34 coils. As can be seen in this figure, all the coils exhibit a maximum heat flux at a length of 1.7 m. In other words, an increasing thermal flux is observed up to this point beyond which the thermal flux decreases in all the coils. Moreover, as can be distinguished in this picture the maximum heat flux has the lowest value in the first coil and assumes its highest amount in the 20th coil. In addition to that, the heat flux increases from the first coil to the 20th and decreases henceforth. Such a trend is due to the difference in the amount of energy absorbed by different coils upon the heat release from the combustion chamber. In more details, the internal coils absorb more from all the burners and as we move to more external coils the absorption becomes less. On the contrary, by considering the heat flux distribution in the curved section of the coils we can say that the thermal flux variations are coherent for all the coils. (The curve section is the range of 8.7-13.9 m of length of the tubes). This is because of a significant distance between this section and the burners which in turn fades out the effect of relative coil location on the tube bank.

Figure 8 (b) gives a picture of temperature distribution on the surface of the tubes for all the coils. As one can see all the coils have two maxima on their tube surface, one in the first vertical compartment and the other one in the second vertical compartment at a height 1.7 m from the bottom of the furnace which results from the maximum thermal flux occurring at these points. Furthermore, this figure demonstrates that the largest and smallest temperature variation ranges belong to the 20th and the first coil.

In order to evaluate the simulation results, we compared them with the experimental results obtained from thermocouples (Tube skin thermocouple) located at a height 5.1 m from the bottom of the furnace on both sides of the 5th and 29th coils (Table 3). As it is clear, the modeling results match those obtained experimentally.

4. Conclusions

The best well-known models, namely Lobo-Evans and Lobo-Evans with gas temperature gradients are based on some simplifying assumptions. The definition of effective cold plane surface area (i.e. αA_{cp} coefficient) or assuming the homogenous thermal flux in the length and height of the furnace are some examples for those simplifications.

Despite numerous advantages, it is essential to note that the Lobo-Evans model is not able to locate the hot spots on the tubes or cannot consider the effects of burner layout in the variations of heat flux patterns. In the Lobo-Evans model burners are replaced with a radiating plane, which results in considering the homogenous heat flux in the combustion. It is evident that such assumption cannot simulate the effects of different burner layouts or individual burner specifications such as: different flame lengths or different fuels fired in each burner. In the Talmor model each burner is replaced by a point heat source rather than a plane source. In this way, the effects of each burner can be considered separately in simulation of the combustion chamber. In the Talmor model the equations are derived for the combustion zone of each burner. Since in the combustion zone, the dominant form of heat transfer is the direct radiation from the flame, one may neglect the effects of the wall radiations or heat transfer due to the circulation of combustion gases. Naturally, by applying this assumption to the upper parts of the combustion chamber, which are out of the combustion zone, may result in some inaccuracies. However, practical comparisons in many cases [29] demonstrate that the mentioned assumptions would lead to an acceptable margin of error in calculating tube skin temperatures in various sections of the fire box.

In the current study, we have simulated heat flux in combustion chamber of a

furnace with arbor coils using the method proposed by Talmor. Subsequent to modeling this furnace, which was assumed to have 7 up-firing burners at the firebox floor, we predicted a maximum heat flux on the 20th coil at a height 1.7 m from the bottom of the furnace with a value 37.4396 kW/m^2, which was less than the maximum permissible heat flux. Furthermore, the maximum temperature on the tube surfaces occurred at a length of 21 m or at a height of 1.7 m from the bottom of the furnace in the second vertical compartment, the value

of which was 567.1°C. These spots correspond to the highest thermal flux absorbed. Close inspection of the temperature distribution for all the coils reveals that simulation results correspond to those obtained experimentally. This model presents a method for direct estimation of the magnitude and location of the hot spot for various furnace design and flame lengths and can also be extended to multiple burner arrangements for the calculation of the hot s pot in a similar fashion.

Nomenclature

A	Cross-sectional area of the combustion zone at distance ξ from the start of combustion	Q_L	Total heat generated by the flame
A_0	Burner tile cross-sectional area	q	Local tube-wall heat flux based on the outside area
A_L	Burner cross-sectional area at $\xi = L$	R	Clearance between burner center and tube face
D_i	Internal diameter of tube	V_L	Volume of the burner
D_o	Outside diameter of tube	x	Location of a point along the length of the tube
f	Flame emissivity	y	Radius of the curved section
K	Combustion coefficient	α	Angular radius of the curved section with the horizontal plane
L	Length of combustion zone	ξ	Distance along the combustion zone from the start of combustion
l	Total length of arbor coil	ξ_0	Distance from A_0 to the apex of a cone or pyramid formed by A_0 and A_L
MW	Molecular weight of fuel gas		

References

1. Hottel, H.C. and Sarofim, A.F. (1967). "Radiative Heat Transfer." Mc Graw –Hill Pub. Co., New York.

2. Hottel, H.C. and Cohen, H.S. (1958). "Radiant Heat Exchange in a gas filled enclosure Allowance for nonuniformity of gas temp." A.I.Ch.E. Journal, Vol. 4, No. 1, pp. 3-14.

3. Nobel, J.M. (1975). "The zone method: Explicit matrix relations for total exchange areas." International Journal of Heat and Mass Transfer, Vol. 18, No. 2, pp. 261-269.

4. Yuen, W. W. and Takara, E. E. (1994). "Development of a generalized zonal method for analysis of radiative transfer in absorbing an an isotropically scattering media." Numerical Heat Transfer, Vol. 25, No. 1, pp. 75-96.

5. Marino, P. (2000). "Numerical Modeling of Steel Tube Reheating in Walking Beam Furnaces." Proceedings of The 5th European Conference on Industrial Furnaces and Boilers, Porto, Portugal, pp. 11-14.

6. Mechi, R., Habib, F. and Said, R. (2007). "Improved zonal method predictions in a rectangular furnace by smoothing the exchange areas." Turkish J. Eng. Env. Sci., Vol. 31, No. 6, pp. 333- 343.

7. Ebrahimi, H., Zamaniyan, A., Soltan Mohammadzadeh, J.S., Khalili, A.A. (2013). "Zonal modeling of radiative heat transfer in industrial furnaces using simplified model for exchange area calculation." Applied Mathematical Modelling, Vol. 37, No. 16-17, pp. 8004- 8015.

8. Tan, C.K., Jenkins, J., Ward, J., Broughton, J. and Heeley, A. (2013). "Zone modelling of the thermal performances of a large-scale bloom reheating furnace." Applied Thermal Engineering, Vol. 50, No. 1, pp. 1111-1118.

9. Fleck Jr., J.A. and Canfield, E.H., (1984). "A random walk procedure for improving the computational efficiency of the implicit Monte Carlo method for nonlinear radiation transport." Journal of Computational Physics., Vol. 54, No. 3, pp. 508–523.

10. Howell, J. R. and Pelmutter, M. (1964). "Monte Carlo Solution of thermal transfer through radiant media between gray walls." ASME Journal of Heat Transfer., Vol. 86, No. 1, pp. 116-122.

11. Howell, J. R. and Pelmutter, M. (1964). "Radiant heat transfer through gray gas between concentric cylinders using Monte Carlo." ASME Journal of Heat Transfer, Vol. 86, No. 2, pp. 169- 179.

12. Steward, F.R. and Cannon, P. (1971). "The calculation of radiative heat flux in a cylindrical furnace using the Monte Carlo method." International Journal of Heat and Mass Transfer., Vol. 14, No. 2, pp. 245-262.

13. Abed, A. Al. and Sacadura, J. F. (1983). "A Monte Carlo finite difference method for coupled radiation – conduction heat transfer in semi transparent media." ASME Journal of Heat Transfer, Vol. 105, No. 4, pp. 931- 933.

14. Tiwari, S. N. and Liu, J. (1992). "Investigation of radiative interaction in laminar flows of non gray gases using Monte Carlo simulation." In Proceeding of the National Heat Transfer Conference, San diego, CA, USA, pp. 187-195.

15. Farmer, J.T. and Howell, J.R. (1994). "Monte Carlo prediction of radiative heat transfer in inhomogeneous, anisotropic, non gray media." Journal of Thermophysics and Heat Transfer, Vol. 8, No. 1, pp. 133- 139.

16. Mishara, S.C. and Blank, D.A.(1995). "High to low optical thickness Monte Carlo solutions of the radiative heat transfer problems in 2-D rectangular enclosures with absorbing- emitting- isotropic scattering." In Proceeding of the International Conference on Advance in Mechanical Engineering, I.I.Sc. Bangalore, India, pp. 1657- 1668.

17. Zhou, Y.H., Shen, Y. J. , Zhang, Z. M., Tsai, B.K. and DeWitt, D.P. (2002). "A Monte Carlo model for predicting the effective emissivity of the silicon wafer in rapid thermal processing furnaces." International Journal of Heat and Mass Transfer, Vol. 45, No.9, pp. 1945- 1949.

18. Soroka, B., Zgurskyy, V. and Pyanykh, K. (2003). "Development of the Monte-Carlo method to predict radiative heat transfer within the boilers and furnaces." 13th Intern. Conference on Thermal Engineering and Thermogrammetry, Budapest, Hungary, pp. 18-20.

19. Maurente, A., Bayer, P. O. and Franca, F. H. R. (2008). "A Monte Carlo Implementation to Solve Radiation Heat Transfer in Non-Uniform Media with Spectrally Dependent Properties." Journal of Quantitative Spectroscopy & Radiative Transfer, Vol. 108, No. 2, pp. 295-307.

20. Kovtanyuk, A.E., Botkin, N.D. and Hoffmann, K.H. (2012). "Numerical simulations of a coupled radiative–conductive heat transfer model using a modified Monte Carlo method." International Journal of Heat and Mass Transfer, Vol. 55, No. 4, pp. 649- 654.

21. Razzaque, M.M., Klein, D.E. and Howell, j.R. (1983). "Finite element solution of radiative heat transfer in a two- dimensional rectangular enclosures with gray participating media." Journal of Heat Transfer, Vol. 105, No. 4, pp. 933- 936.

22. Razzaque, M.M., Howell, J.R. and Klein, D.E. (1984). "Coupled radiative and conductive heat transfer in two- dimensional enclosure with gray participating media using finite elements." Journal of Heat Transfer, Vol. 106, No. 3, pp. 613- 619.

23. Chung, T.J. and Kim, J.Y. Two-Dimensional, (1984). "Combined-Mode Heat Transfer by Conduction, Convection, and Radiation in Emitting, Absorbing, and Scattering Media-Solution by Finite Elements." Journal of Heat Transfer, Vol. 106, No. 2, pp. 448- 452.

24. Fernandes, R., Francis, J. and Reddy, J. (1980). "A finite element approach to combined conductive and radiative heat transfer in a planar medium." 15th Thermophysics Conference, Snowmass,CO,U.S.A.

25. Fernandes, R. and Francis, J. (1982). "Combined Conductive and Radiative Heat Transfer in an Absorbing, Emitting, and Scattering Cylindrical Medium." Journal of Heat Transfer, Vol. 104, No. 4, pp. 594-601.

26. Harish, J. and Dutta, P. (2005). "Heat transfer analysis of pusher type reheat furnace." Ironmaking and Steelmaking , Vol. 32, No. 2, pp. 151–158.

27. Kim, M. Y. (2007). "A heat transfer model for the analysis of transient heating of the slab in a direct–fired walking beam type reheating furnace." International Journal of Heat and Mass Transfer, Vol. 50, No. 19-20, pp. 3740–3748.

28. Hachem, E., Jannoun, G., Veysset, J., Henri, M., Pierrot, R., Poitrault, I., Massoni, E. and Coupes, T. (2013). "Modeling of heat transfer and turbulent flow inside industrial furnaces." Simulation Modeling Practice and Theory, Vol. 30, pp. 35- 53.

29. Talmor, E. (1982). "Combustion Hot Spot Analysis for Fired Process Heaters." Gulf Publishing Co.,Houston, Texas.

30. Prasanna, D. and Aung, K. (2006). "Combustion Hot Spot Analysis for Single-Side-Fired Tubes In a Floor-Fired Box Furnace." ASME International Mechanical Engineering Congress and Exposition, Chicago, Illinois, USA.